Retroreflection with Amplification for Long Range mmWave Sensing

Siddharth Mohan, Kshitiz Bansal, Manideep Dunna, Dinesh Bharadia
University of California San Diego

ABSTRACT

Millimeter wave sensing has rapidly gained prominence with the advent of Frequency Modulated Continuous Wave (FMCW) radars, redefining applications in both indoor and outdoor domains. An emerging focus in this field revolves around developing intelligent infrastructure tags, which serve as fiducials for these radars, enabling easy and accurate identification. Leveraging specialized antenna architecture and modulation techniques, these tags enhance detectability and identification performance. Moreover, this system allows for real-time signal detection without the need for additional communication systems. However, a critical challenge lies in ensuring the reliable detection of these tags, particularly in terms of their operational range. This research addresses this challenge by introducing a conceptual tag operating at the millimeter wave frequency of 24 GHz. The tag incorporates a switch and an amplifier, effectively improving the SNR of the tag. As a result, the overall operational range of the tags improves significantly, as well as the detection rate at shorter distances. Hence, by improving the SNR of these tags, the amplifier represents a crucial advancement in enhancing the system's reliability in detecting these tags. Simulated results clearly show the feasibility and potential of this proposed solution, paving the way for robust and dependable mmWave tag systems in various applications.

CCS CONCEPTS

• **Hardware → PCB design and layout**; • **Networks → Error detection and error correction**.

KEYWORDS

Radar, FMCW, Amplifier, Switch, mmWave,Range

ACM Reference Format:
Siddharth Mohan, Kshitiz Bansal, Manideep Dunna, Dinesh Bharadia. 2023. Retroreflection with Amplification for Long Range mmWave Sensing. In *The 7th ACM Workshop on Millimeter-Wave and Terahertz Networks and Sensing Systems (mmNets '23), October 06, 2023, Madrid, Spain.* ACM, New York, NY, USA, 7 pages. https://doi.org/10.1145/3615360.3625090

1 INTRODUCTION

Millimeter wave (mmWave) radar sensing has witnessed significant advancements, permeating various indoor and outdoor applications, owing to its environmental agnosticism compared to visual sensing approaches. The breadth of its utilization spans from indoor scenarios encompassing people counting [1], building security [2], smart home systems [3, 4], and health monitoring [5, 6], to outdoor domains including blind spot detection [7], adaptive cruise control [8], traffic monitoring [9], and drone perception [10].

However, mmWave transmissions present significant challenges due to higher path loss compared to lower frequency bands, alongside the issues of specular reflections and limited resolution [11, 12]. These challenges have hindered the effective use of mmWave signals and radars for object sensing and identification tasks, such as detecting traffic signs. To overcome these obstacles, researchers have explored various types of millimeter wave backscatter tags [13–18], designed to facilitate concurrent data communication and identification among multiple tags.

Notably, the backscatter tags described in studies such as [13] have demonstrated their potential by enabling widespread deployment on existing traffic infrastructure or vehicles, allowing the detection of traffic signs and dynamic objects, even in adverse weather conditions, using commercial-off-the-shelf (COTS) automotive radars. These tags employ multiple antennas based on the van-Atta array architecture, ensuring robust radar reflections regardless of the incidence angle. However, existing mmWave tags, including those discussed in [13–17], have limited detection ranges, typically under 30 meters. Despite serving as a promising foundation, achieving

1

more extensive ranges remains essential for robust and reliable object detection. This requirement is especially crucial for enhancing the capabilities of automotive Frequency Modulated Continuous Wave (FMCW) radars, both indoors and outdoors.

This paper aims to address this challenge by focusing on extending the range of mmWave backscatter tags for long-distance sensing, while ensuring compatibility with all types of mmWave radars. The proposed work is poised to enhance both outdoor and indoor sensing capabilities, particularly by augmenting the range of automotive FMCW radars for detecting infrastructure elements using mmwave backscatter tags. Through this research, we aim to bolster the overall efficacy and practicality of mmWave tag systems, fostering improved object detection and identification in diverse scenarios.

The paper is organized as follows: Section 2 describes the tag's design using the amplifier. Simulated results are provided in Section 3. Finally, the conclusions are included in Section 4.

2 BACKGROUND AND MOTIVATION

With the advancements in mmWave backscatter systems, a need arises to address the inherent path loss introduced by the transmission medium. As the signal frequency increases, the path loss or reduction in signal strength becomes more pronounced for a given distance. This effect is particularly evident in mmWave signals, which operate from 24 GHz to 100 GHz, experiencing higher path loss compared to lower frequency signals like WiFi. To compensate for this loss, specialized antenna architectures are required for backscatter tags operating at these frequencies [14]. These architectures aim to focus more energy back towards the receiver, mitigating the effects of signal loss.

One such architecture utilized in mmWave tags is the Van Atta array concept [19, 20], where incident RF signals are reflected back in the same direction. In Van Atta architecture, pairs of antennas are interconnected through transmission lines. The path lengths connecting the antennas are designed to have a length difference equal to an integer multiple of the wavelength. This arrangement leads to the generation of reversed phases at the antenna array, resulting in retroreflectivity, where the signal is reflected back in the direction of incidence.

To provide unique identification to the tags, RF switches are commonly employed. These switches allow for the toggling between Van Atta and absorbing states. When the RF switch is turned on, the connection between the antenna pairs is established, enabling retroreflection and providing a high radar cross-section (RCS) to the radar where RCS is a proxy for the strength of reflections from an object [13]. Conversely, when the RF switch is turned off, the transmission line ends are terminated in a 50-ohm resistor, causing the incident signal to be completely absorbed by the tag and resulting in a lower RCS. By modulating the switching state of the RF switch in an ON-OFF scheme, the tag can convey information through fluctuations in the RCS, allowing the radar to discern the transmitted information.

Despite leveraging Van Atta-based retroreflectivity and increasing the number of antenna elements, the achievable range of these mmWave tags remains limited to within a few hundred meters, that too for 24 GHz radars [16]. For 77 GHz radars, the maximum range reported is much lesser (within 10m) [21]. Moreover, the RF switches used in these systems introduce additional losses, further reducing the effective range of operation. This limitation poses a significant challenge, especially for applications in diverse indoor and outdoor scenarios, such as automotive radar systems operating at higher frequencies like 77 GHz. Simply increasing the number of antenna elements reaches a point of diminishing returns in terms of range enhancement.

Motivated by the need for extended tag range capabilities, particularly in critical applications like automotive systems, this paper presents the concept of amplification using a low-noise amplifier as a proof of concept. The aim is to demonstrate how incorporating amplification can enhance the range of mmWave tags by multiple folds. Figure 1 shows the improved tag ranges for different LNA gains. By showcasing the potential benefits of this approach, we seek to advance the capabilities of mmWave tag systems, enabling robust and reliable long-distance sensing in various application domains.

3 DESIGN & IMPLEMENTATION

3.1 Tag Components

The tag consists of an RF switch whose input and output are connected to a pair of series-fed patch array antennas. The signal received by the antennas passes through the switch, which can either redirect it to the ground or

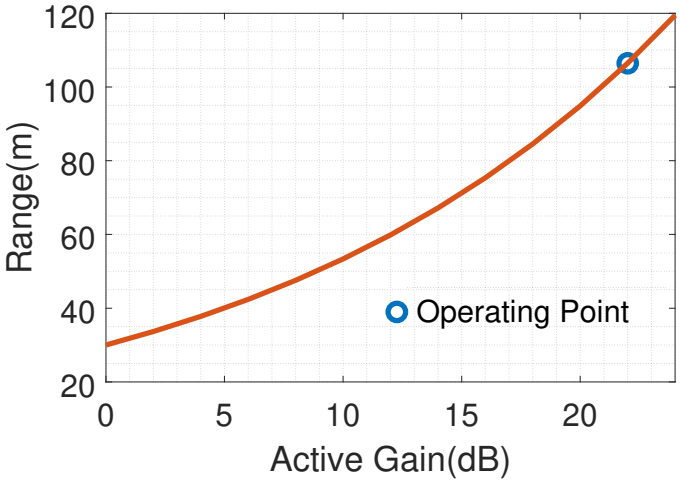

Figure 1: Tag Range vs Active gain from Amplification

let it pass to output antennas (Figure 1). This switching creates ON and OFF states of the tags, achieving modulation. To increase the power of the output signal, we propose to use a mmWave Low Noise Amplifier (LNA) in series with the RF switch. The signal from the radar is received by the input antenna, which is then amplified and re-transmitted through the output antenna, hence achieving retroreflection with amplification. One of the main design considerations is the antenna performance in terms of the gain and matching. The antenna array has been designed to operate in the ISM band, and this process required fine-tuning of the antenna patch dimensions and their interconnecting traces.

To showcase the concept, we choose the base tag design of R-fiducial [13]. This tag is designed for a 24 GHz radar and shows a maximum range of up to 25m. The choice of the amplifier is highly important in this system. The amplifier we use in our work is a high dynamic range GaAs pHEMT MMIC (Monolithic Microwave Integrated Circuit) LNA which operates in the 17GHz to 27GHz frequency band. Its current consumption is 73 mA at 4 V, and it has a typical gain of more than 22 dB at 24GHz. The switch used is low insertion loss (1.1dB), high isolation ($\sim$ 38 dB) at 24GHz. The system is designed to cover the 24.25 GHz ISM (Industrial, Scientific, Medical) band.

3.2 Decoupling Control from the RF board in the Tag

An important consideration of our design is to decouple the RF circuitry from the controller circuitry. The printed circuit board (PCB) design for the system was done to keep the RF (Antenna) and Digital (Controller) sections separate. The RF board incorporates the Antenna, LNA, and the RF Switch as illustrated in Figure 2. The control circuit, as shown in Figure 3, controls the RF switch on the tag for which we use an onboard PSoC 6 MCU (Microcontroller unit). We implement two Linear feedback shift registers (LFSR) on the MCU to generate the gold code sequence. The generated bits are outputted from a GPIO pin and are fed to the RF switch as the control signal. The LFSRs can be configured to use different length codes. In our implementation, we use 5-bit LFSRs to generate 32-bit codes.

Figure 4 shows how the two boards plug into each other. Separating the RF & Control boards provides the flexibility of using other antenna modules with the same controller board. This is advantageous in terms of manufacturability, reusability, and even for debugging purposes. We can try multiple antenna modules, including off-the-shelf parts, to compare performance without changing the control section. This can also help to debug issues with variations across RF boards due to manufacturing because, at such high frequencies, even slight variations in the patch antenna sizes can lead to major performance deviations. This also allows for a faster turnaround time if design changes are required only on the RF board. One can make the design changes to the RF section without worrying about refabricating the controller board. All this would have been challenging if both the RF and Control sections were on the same board, though at the minor cost of maintaining two separate boards.

3.3 PCB design considerations

3.3.1 Choosing the right substrate. At mmwave frequencies, the RF signal is quite sensitive to the material used to manufacture the PCBs. Hence, it becomes extremely important to choose the right substrate for any given frequency. Our PCBs utilize Rogers 4003C dielectric as a substrate to minimize the RF trace losses at mmWave frequencies. Rogers 4003C is a well-known circuit board laminate material designed for high-frequency applications up to gigahertz frequencies. RO4003C laminates provide tight control on dielectric constant (Dk) and low loss while leveraging the same processing method as standard epoxy but at a fraction of the cost of conventional microwave laminates. It has a stable dielectric

constant of 3.38 +/- 0.05 and a dissipation factor of 0.0027 at 10 GHz.

3.3.2 Solder Mask. It is important to do the board layout cautiously, considering the signal distortion that can occur at such a high frequency. For this reason, the solder mask has been avoided or etched out of the top layer in and around the antenna array, as can be seen in Figure 5. This also helps to reduce the fabrication process variability. Further, due to the intrinsic solder mask qualities, there are numerous reasons to avoid solder mask coverage on RF conductors. Liquid photo imageable (LPI), which typically has a high dissipation factor (Df) and high moisture absorption, is the most common type of solder mask used in the PCB industry. The thickness of the LPI solder mask can vary depending on the processing or design. The circuit's dielectric loss is increased by the solder mask's higher Df characteristic, which also enhances insertion loss.

Another thing to keep in mind is that typically grounded coplanar waveguide (GCPW) or microstrip structures are used for RF circuitry on a PCB's outer layer, including our design. Now, the medium that has the lowest loss for electromagnetic waves is air. Thus, due to the use of air by their fields, both GCPW and microstrip structures can benefit from lower insertion loss. In cases where GCPW or microstrip is covered in a solder mask, some of the fields that previously used air as the dielectric medium will then employ a solder mask, thereby degrading the signal performance. In addition to this, stitching vias have specifically been avoided around the traces feeding the antenna chains based upon past experience where manufacturing tolerances caused problems with trace impedance.

3.3.3 Trace length matching. From the board design perspective, after including the LNA, the trace lengths had to be modified such that the path lengths from the antenna array chain maintain the Van Atta array properties, that is, the length of the trace connecting the antenna chain to the LNA on one side is the same as that connecting the opposite antenna chain to the respective series switch. The trace widths of the antenna array were also modified for fine-tuning impedance matching and, thereby, the resonance frequency. Multiple parametric simulations were run to come up with the fine-tuned dimensions. In mmWave applications, even minor changes in dimensions can offset the resonance frequency; hence, we targeted to have an S11 of -10dB or below in the band from 23.7Ghz to 24.2Ghz.

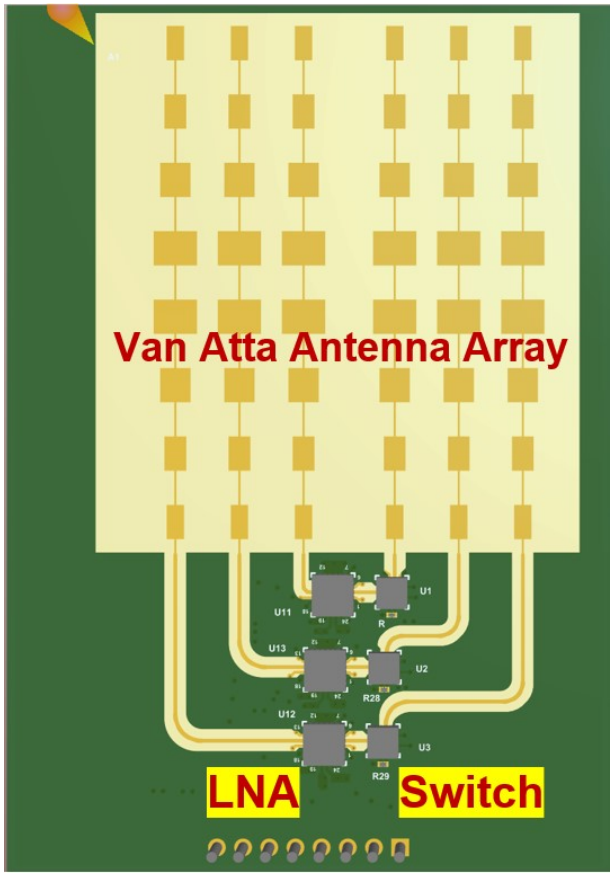

Figure 2: RF Board with Antenna, Switch and LNA

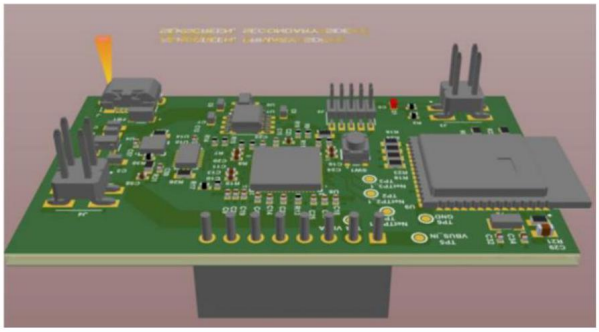

Figure 3: Controller board with MCU

4 TAG ANALYSIS

4.1 Loss benchmarks

Following the conceptual design proposed in the previous section, the antenna simulations were performed in Ansys HFSS electromagnetic solver to ensure good

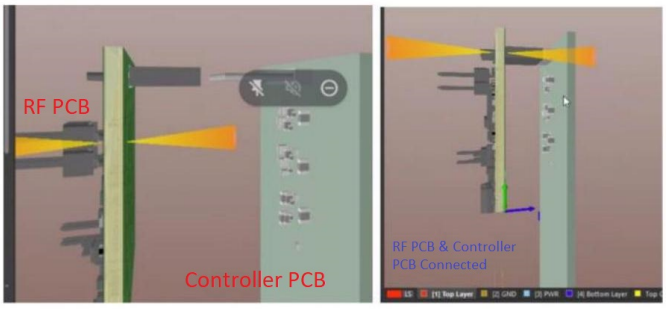

Figure 4: RF Board and Controller board pluggability

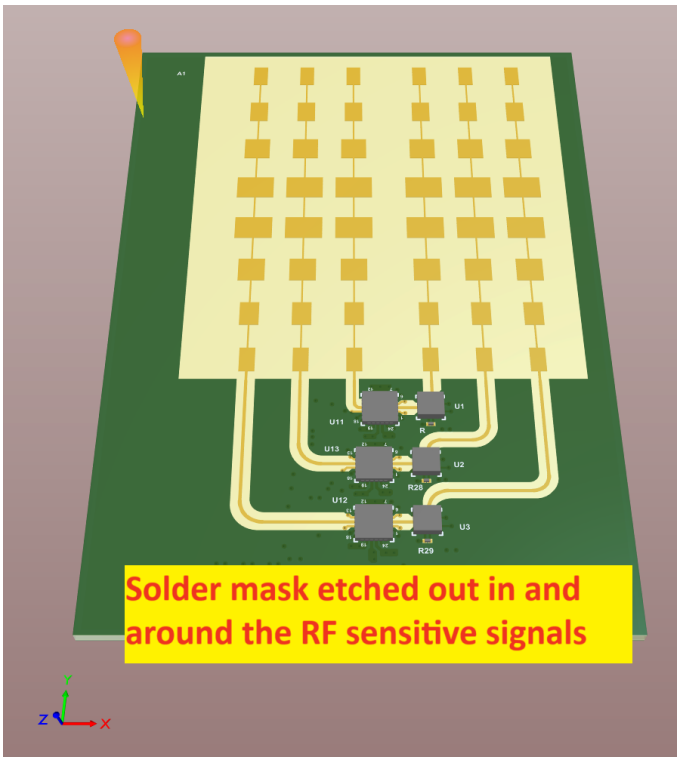

Figure 5: Solder mask has been etched out in and around the antenna array as well as around the traces feeding them

return loss and gain in the 24 – 24.25GHz ISM operating frequency band. Results are shown in Figure 6 and Figure 7. Figure 6 shows the S11(return loss) to be much better than -10dB in the band of operation, and Figure 7 shows the antenna array gain to be more than 12 dB. The antenna S-parameters were then extracted and used in conjunction with LNA and switch S-parameters to check the overall system performance through S-parameters analysis in Keysight ADS software, results of which are shown in Figure 8. As indicated by the S21 plot in Figure 8, even with the switch and antenna losses, we are able to maintain a gain of close to 18 dB to 20 dB.

4.2 Range Improvement

To estimate the range improvements with the proposed design, we performed an approximate range analysis using the radar range equation 1 as shown below where $P_r, P_t, G_t, G_r, \lambda, d$ and σ are the received signal strength (RSS), transmit (Tx) signal power, Tx gain, receive (Rx) gain, signal wavelength in free space, radar-to-object distance, and the Radar Cross Section (RCS) of the object, respectively [21]. This equation applies to a typical monostatic radar, i.e., the Tx and Rx antennas are colocated. The RSS level P_r is directly proportional to wavelength λ, posing a challenge at mmWave frequencies which suffer from higher attenuation loss given their smaller wavelengths.

$$P_r = \frac{P_t G_t G_r \lambda^2 \sigma}{(4\pi)^3 d^4} \quad (1)$$

Approximate calculations show a range increase of more than three times with the usage of a single LNA per branch of the antenna array. So, if we consider previous work done as illustrated in [13–15] with tag's range to be around 25 m the new range will be over 75 m. The higher the amplifier gain, the lower the switch insertion loss the better the range. Note that this design would be compatible with most of the existing tag architectures [13–17] showing a significant boost in range and SNR of signal.

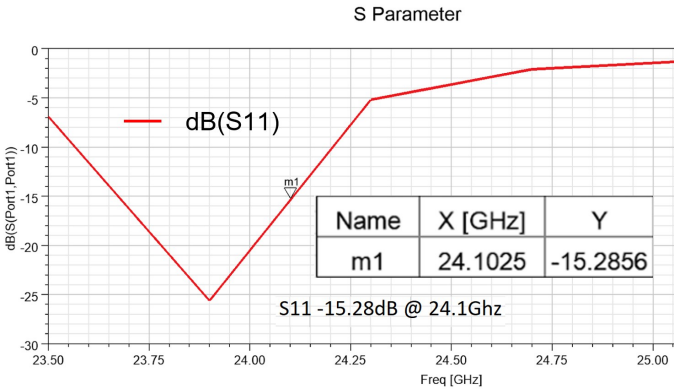

Figure 6: Antenna simulation results in Ansys HFSS with Return Loss peaking around 24.1GHz

5 CONCLUSION

In conclusion, this paper discusses the concept of mmwave backscatter tags with amplification for long-range mmWave sensing, increasing the detection range by at least three times their existing values. For the same tag to radar separation, the SNR increases because of amplification,

5

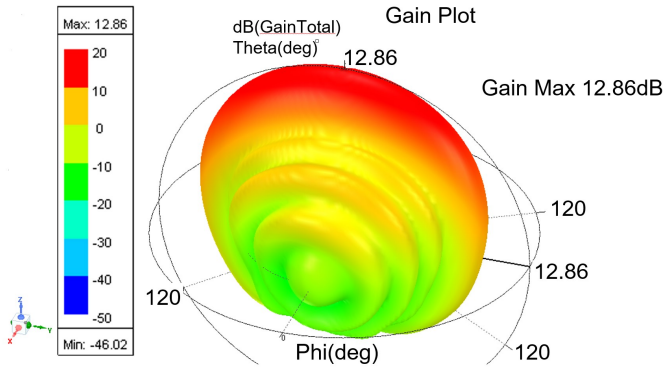

Figure 7: Gain Plot showing a gain of more than 12dB

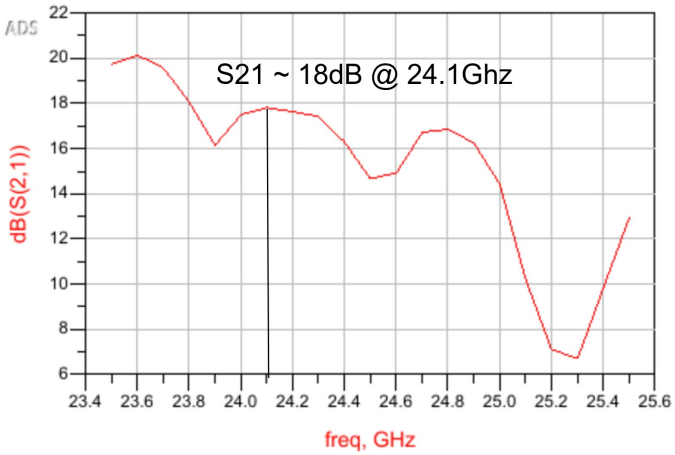

Figure 8: LNA + Switch + Antenna simulation results in Keysight ADS

hence decreasing the probability of detection failure, thereby increasing the system's reliability. This can be achieved by using active components like amplifiers with passive antenna arrays in conjugation with switches to provide modulation. The work presented in this paper is primarily based on simulations through the evaluation boards already designed. In future work, we plan to measure the fabricated prototype in different indoor and outdoor scenarios to test the range enhancement. Hardware evaluation will help to understand any shortcomings that the simulations might have as well as to improve the future versions of the design. We also wish to look into the possibility of varying the gain of the amplifier to check for the impact of both higher and lower gain on the detection range.

REFERENCES

[1] Jonas Weiß, Rodrigo Pérez, and Erwin Biebl. Improved people counting algorithm for indoor environments using 60 ghz fmcw radar. In *2020 IEEE Radar Conference (RadarConf20)*, pages 1–6. IEEE, 2020.

[2] S Stanko, D Notel, A Wahlen, J Huck, F Kloppel, R Sommer, M Hagelen, and H Essen. Active and passive mm-wave imaging for concealed weapon detection and surveillance. In *2008 33rd International Conference on Infrared, Millimeter and Terahertz Waves*, pages 1–2. IEEE, 2008.

[3] Yudi Dong and Yu-Dong Yao. Secure mmwave-radar-based speaker verification for iot smart home. *IEEE Internet of Things Journal*, 8(5):3500–3511, 2020.

[4] Haipeng Liu, Yuheng Wang, Anfu Zhou, Hanyue He, Wei Wang, Kunpeng Wang, Peilin Pan, Yixuan Lu, Liang Liu, and Huadong Ma. Real-time arm gesture recognition in smart home scenarios via millimeter wave sensing. *Proceedings of the ACM on interactive, mobile, wearable and ubiquitous technologies*, 4(4):1–28, 2020.

[5] Mostafa Alizadeh, George Shaker, João Carlos Martins De Almeida, Plinio Pelegrini Morita, and Safeddin Safavi-Naeini. Remote monitoring of human vital signs using mm-wave fmcw radar. *IEEE Access*, 7:54958–54968, 2019.

[6] Peijun Zhao, Chris Xiaoxuan Lu, Bing Wang, Changhao Chen, Linhai Xie, Mengyu Wang, Niki Trigoni, and Andrew Markham. Heart rate sensing with a robot mounted mmwave radar. In *2020 IEEE International Conference on Robotics and Automation (ICRA)*, pages 2812–2818. IEEE, 2020.

[7] Guiru Liu, Mingzheng Zhou, Lulin Wang, Hai Wang, and Xiansheng Guo. A blind spot detection and warning system based on millimeter wave radar for driver assistance. *Optik*, 135:353–365, 2017.

[8] Hiroshi Kuroda. An adaptive cruise control system using a millimeter wave radar. In *IEEE International Conference on Intelligent Vehicles. Proceedings of the 1998 IEEE International Conference on Intelligent Vehicles*, volume 1, 1998.

[9] Feng Jin, Arindam Sengupta, Siyang Cao, and Yao-Jan Wu. Mmwave radar point cloud segmentation using gmm in multimodal traffic monitoring. In *2020 IEEE International Radar Conference (RADAR)*, pages 732–737. IEEE, 2020.

[10] Sedat Dogru and Lino Marques. Pursuing drones with drones using millimeter wave radar. *IEEE Robotics and Automation Letters*, 5(3):4156–4163, 2020.

[11] Kshitiz Bansal, Keshav Rungta, Siyuan Zhu, and Dinesh Bharadia. Pointillism: Accurate 3d bounding box estimation with multi-radars. In *Proceedings of the 18th Conference on Embedded Networked Sensor Systems*, pages 340–353, 2020.

[12] Kshitiz Bansal, Keshav Rungta, and Dinesh Bharadia. Radsegnet: A reliable approach to radar camera fusion. *arXiv preprint arXiv:2208.03849*, 2022.

[13] Kshitiz Bansal, Manideep Dunna, Sanjeev Anthia Ganesh, Eamon Patamsing, and Dinesh Bharadia. R-fiducial: Reliable and scalable radar fiducials for smart mmwave sensing. *arXiv preprint arXiv:2209.13109*, 2022.

[14] Mohammad Hossein Mazaheri, Alex Chen, and Omid Abari. Mmtag: A millimeter wave backscatter network. In *Proceedings of the 2021 ACM SIGCOMM 2021 Conference*, pages 463–474, 2021.

[15] Weilin Chen. Survey of millimeter wave backscatter communition systems. *arXiv preprint arXiv:2305.10302*, 2023.

[16] Elahe Soltanaghaei, Akarsh Prabhakara, Artur Balanuta, Matthew Anderson, Jan M Rabaey, Swarun Kumar, and Anthony Rowe. Millimetro: mmwave retro-reflective tags for accurate, long range localization. In *Proceedings of the 27th Annual International Conference on Mobile Computing and Networking*, pages 69–82, 2021.

[17] Kang Min Bae, Namjo Ahn, Yoon Chae, Parth Pathak, Sung-Min Sohn, and Song Min Kim. Omniscatter: extreme sensitivity mmwave backscattering using commodity fmcw radar. In *Proceedings of the 20th Annual International Conference on Mobile Systems, Applications and Services*, pages 316–329, 2022.

[18] Rohith Reddy Vennam, Ish Kumar Jain, Kshitiz Bansal, Joshua Orozco, Puja Shukla, Aanjhan Ranganathan, and Dinesh Bharadia. mmspoof: Resilient spoofing of automotive millimeter-wave radars using reflect array. In *2023 IEEE Symposium on Security and Privacy (SP)*, pages 1807–1821. IEEE, 2023.

[19] E Sharp and M Diab. Van atta reflector array. *IRE Transactions on Antennas and Propagation*, 8(4):436–438, 1960.

[20] Lester Clare Van Atta. Electromagnetic reflector, October 6 1959. US Patent 2,908,002.

[21] John Nolan, Kun Qian, and Xinyu Zhang. Ros: passive smart surface for roadside-to-vehicle communication. In *Proceedings of the 2021 ACM SIGCOMM 2021 Conference*, pages 165–178, 2021.

7